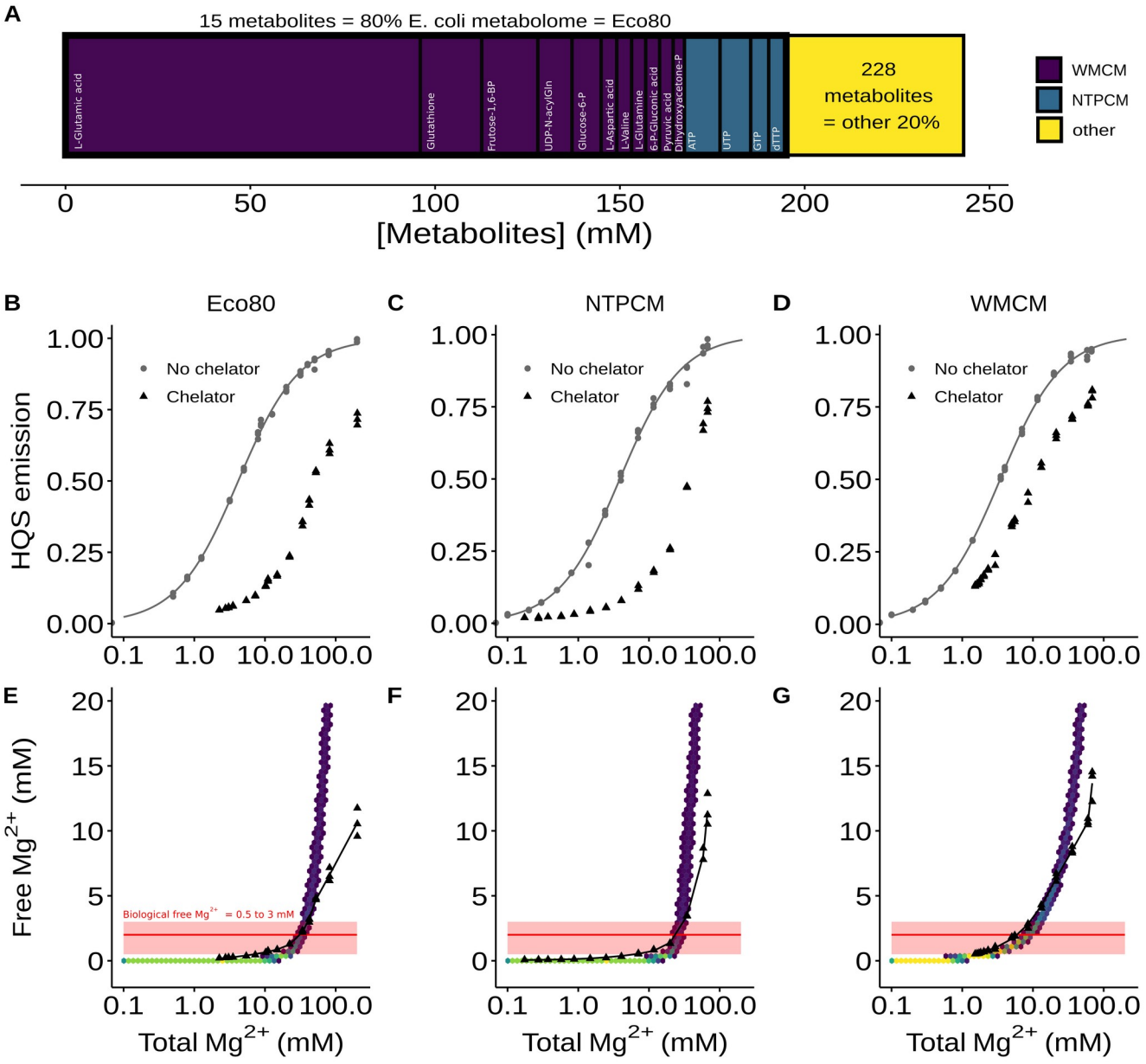

Figure 1 Analysis of Mg^{2+} speciation in *E. coli* metabolite mixtures. Eco80 contains **(A)** E. coli metabolome molar composition. Eco80 contains the 15 most abundant metabolites that comprise 80% of the *E. coli* metabolome. NTPCM contains four strong Mg^{2+} chelating NTPs, and WMCM contains 11 other weak Mg^{2+} binding metabolites. **(B-D)** Effect of Mg^{2+} on 8-hydroxyquinoline-5-sulphonic acid (HQS) emission with and without mixtures of metabolites that chelate Mg^{2+}. Grey lines represent fits to determine the binding constant for Mg^{2+} and HQS in the absence of chelators. **(E-G)** Relationship between the total Mg^{2+} concentration and the free Mg^{2+} concentration with mixtures of metabolites that chelate Mg^{2+}. The free Mg^{2+} concentration (y-axis) was calculated using HQS emission and the binding constant for Mg^{2+} and HQS. Hex bins represent a statistical simulation of 1000 virtual artificial cytoplasms based on experimental errors in K_D determination, experimental errors in reagent concentrations, and single site binding. Triangle data points are free Mg^{2+} concentrations calculated using HQS emission. Black lines were generated using polynomial regression. The red shaded region is the biological free Mg^{2+} concentration, 0.5 to 3 mM. The red line is the approximate free Mg^{2+} concentration in *E. coli*.

Table 1. Eco80: the 15 most abundant metabolites which comprise 80% of the *E. coli* metabolome.

Metabolite	Conc. (mM)	K_D (mM)	Chelation stength
ATP	9.63 (0.963)[a]	0.28 (0.01)b	NTPCM (Strong[e])
UTP	8.29 (0.829)[a]	0.248 (0.004)[b]	NTPCM (Strong[e])
GTP	4.87 (0.487)[a]	0.201 (0.007)[b]	NTPCM (Strong[e])
dTTP	4.62 (0.462)[a]	0.160 (0.003)[b]	NTPCM (Strong[e])
L-Glutamic acid	96 (9.6)[a]	520 (50)[c]	WMCM (Weak[e])
Glutathione	16.6 (1.66)[a]	NA[d]	WMCM (Weak[e])
Fructose 1,6-bisphosphate	15.2 (1.52)[a]	5.9 (0.1)[b]	WMCM (Weak[e])
UDP-N-acytylglucosamine	9.24 (0.924)[a]	29 (2)[b]	WMCM (Weak[e])
Glucose 6-phosphate	7.88 (0.788)[a]	17.3 (0.2)[b]	WMCM (Weak[e])
L-Aspartic acid	4.23 (0.423)[a]	465 (12)[c]	WMCM (Weak[e])
L-Valine	4.02 (0.402)[a]	NA[d]	WMCM (Weak[e])
L-Glutamine	3.81 (0.381)[a]	NA[d]	WMCM (Weak[e])
6-Phospho-gluconic acid	3.77 (0.377)[a]	14.4 (0.2)[b]	WMCM (Weak[e])
Pyruvic acid	3.66 (0.366)[a]	15.8 (0.9)[c]	WMCM (Weak[e])
Dihydroxyacetone phosphate	3.06 (0.306)[a]	20 (1)[b]	WMCM (Weak[e])

[A]uncertainty propagated from uncertainties in reagent masses and volumes used during sample preparation. Extra significant digits included to avoid systematic rounding errors in the statistical model.
[b]Determined at 37 °C with Isothermal titration calorimetry as measured in SI figure 1 and SI table 2. Error is the propagated standard error in the fit parameters.
[c]Determined at 37 °C with HQS emission as measured in the SI figure 2 and SI table 3. Error is the propagated standard error in the fit parameters.
[d]No binding observed as per SI Figure 2.
[e]Metabolites with K_Ds for Mg^{2+} less than 2 mM are considered strong Mg^{2+} chelators.

SI Table 1. Recipe for the Eco80 artificial cytoplasm (Add in later in word when I am formatting the tables)

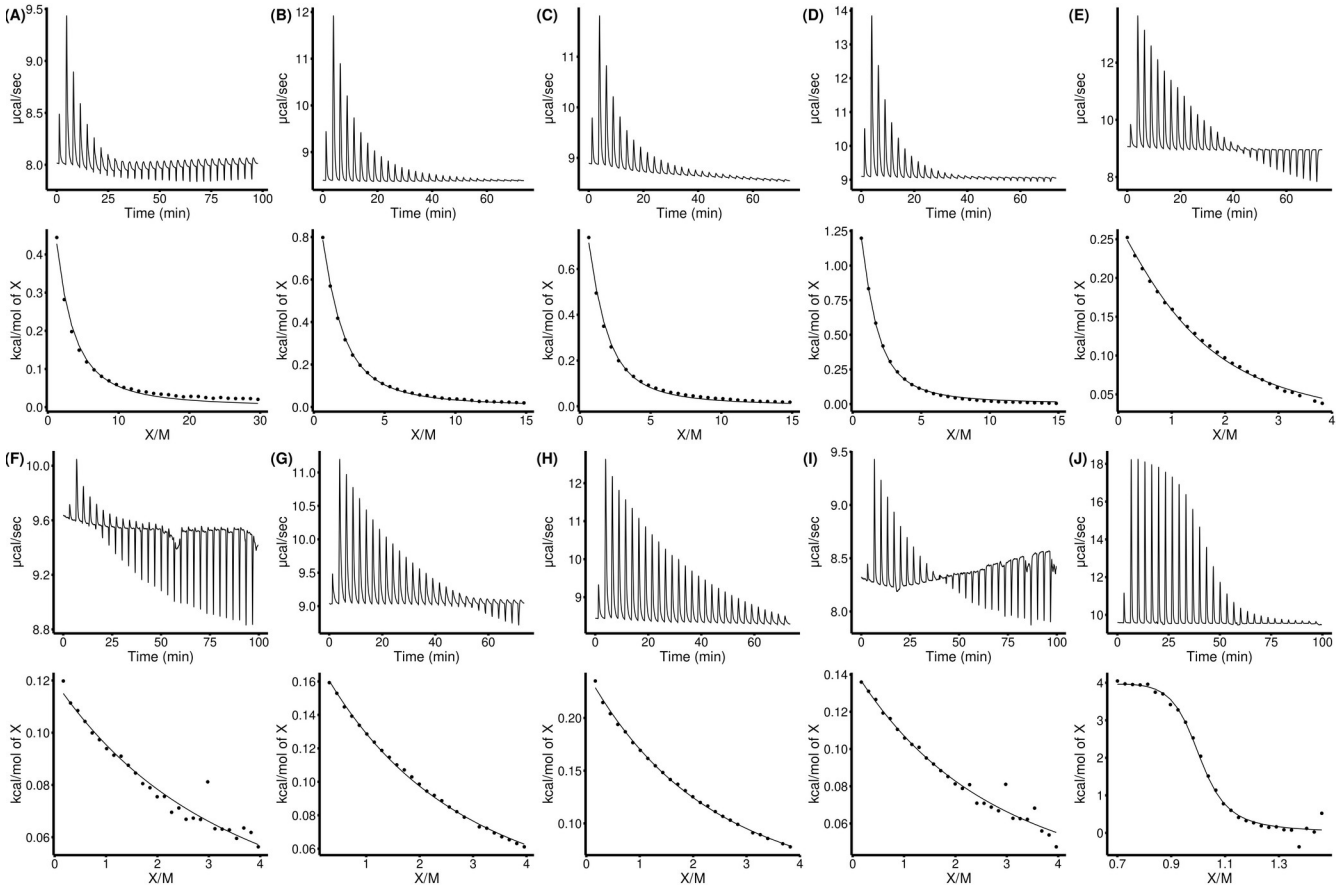

SI Figure 1 Isothermal titration calorimetry (ITC) analysis of Mg^{2+} binding to metabolites in 240 mM NaCl 140 mM KCl 10 mM HEPES pH 7.0 at 37 °C. $MgCl_2$ was titrated into metabolites and the power was monitored over time (Top panel). Heat of the injection was calculated by integrating the raw power curve, and the background heat of $MgCl_2$ diltution, collected on buffer containing no metabolite, was subtracted to produce the isotherms in the bottom panels. Lines in bottom pannels represent fits to the Weismann isotherm equation to determine apparent association constants. **(A)** Adenosine triphosphate (ATP). **(B)** Uridine triphosphosphate (UTP). **(C)** Guanosine triphsophate (GTP). **(D)** deoxythymidine triphosphate (dTTP). **(E)** Fructose 1,6-bisphosphate. **(F)** Uridine diphosphate (UDP)-N-acytylglucosamine. **(G)** Glucose 6-phosphate. **(G)** 6-phosphogluconic acid. **(H)** phosphoenol pyruvate. **(G)** Ethylene diamine-tetracetic acid (EDTA). Thermodynamic values are found in SI table 2.

SI Table 2 Apparent binding constants determined with Isothermal titration calorimetry (ITC).

Metabolite	Syringe (mM)	Cell (mM)	ΔH (kcal/mol)	K' (M^{-1})	K_D' (mM^{-1})
ATP	15 mM $MgCl_2$[a]	0.1 mM ATP[a]	1.83 (0.04)	3600 (200)	0.28 (0.01)
UTP	15 mM $MgCl_2$[a]	0.2 mM UTP[a]	1.70 (0.01)	4200 (70)	0.248 (0.004)
GTP	15 mM $MgCl_2$[a]	0.2 mM GTP[a]	1.43 (0.02)	5000 (200)	0.201 (0.007)
dTTP	15 mM $MgCl_2$[a]	0.2 mM dTTP[a]	2.19 (0.02)	6300 (300)	0.160 (0.003)
Fructose 1,6-BP	100 mM $MgCl_2$[a]	5.0 mM Fructose 1,6-BP[a]	0.414 (0.004)	169 (4)	5.9 (0.1)
UDP-GlcNAC	100 mM $MgCl_2$[a]	5.0 mM UDP-GlcNAC	0.57 (0.02)	34 (2)	29 (2)
Glucose 6-P	100 mM $MgCl_2$[a]	5.0 mM Glucose 6-P[a]	0.555 (0.003)	57.9 (0.7)	17.3 (0.2)
6-P-gluconic acid	100 mM $MgCl_2$[a]	5.0 mM 6-P-gluconic acid[a]	0.662 (0.005)	70 (1)	14.4 (0.2)
Dihydroxyacetone phosphate	100 mM $MgCl_2$[a]	5.0 mM dihydroxy-acetone phosphate[a]	0.50 (0.01)	51 (3)	20 (1)
EDTA	6 mM $MgCl_2$[a]	1.5 mM EDTA 1.0 mM $MgCl_2$[a,b]	2.85 (0.04)	220,000 (30,000)	0.0045 (0.0006)

[a]240 mM NaCl 140 mM KCl 10 mM HEPES pH 7.0 at 37 °C

[b]Mg^{2+} and EDTA were incorporated into the cell in order to sequester trace tight binding metal ions and thereby negate their contribution to ITC signal.

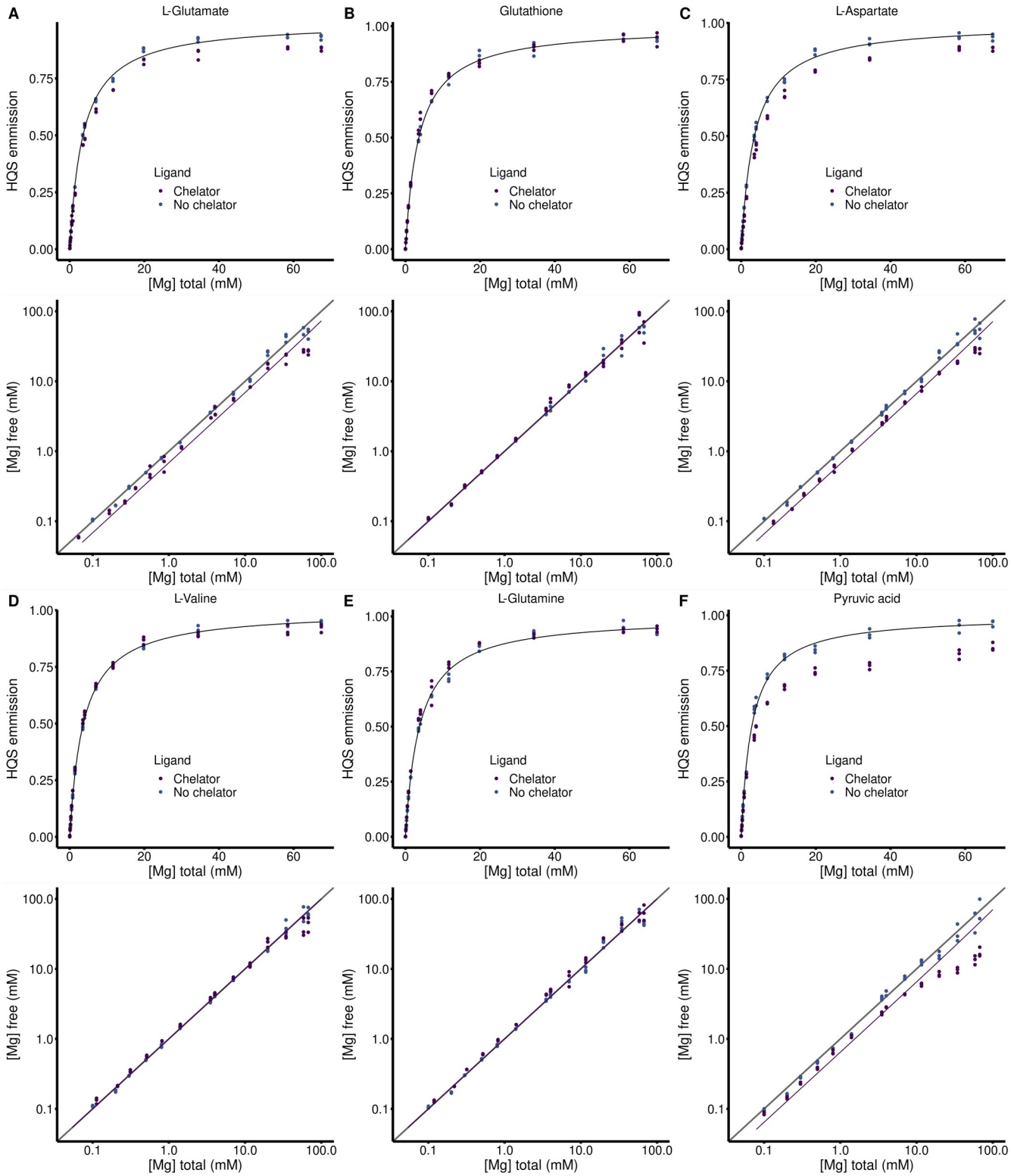

SI Figure 2 HQS analysis of Mg2+ binding to metabolites in 240 mM NaCl 140 mM KCl 20 mM MOPS 0.01 mM EDTA 0.001% SDS pH 7.0. (Top panels) Dependence of HQS emission on the total concentration of $MgCl_2$ in the presence and absence of a metabolite chelators. Black lines represent a fit to SI equation 1 to determine the F_{max}, F_{min}, and K_{HQS}. (Bottom panels) Dependence of the free Mg^{2+} concentration on the total concentration of $MgCl_2$ in the presence and absence of a metabolite chelators. Grey lines represent where the free Mg^{2+} concentration equals the total concentration of $MgCl_2$, Purple lines represent a fit to SI equation 4 to determine the association constant between HQS and a chelator. **(A)**

240 mM L-glutamate. **(B)** 194 Glutathione. **(C)** 240 mM L-aspartate. **(D)** 240 mM L-valine. **(E)** 240 mM L-glutamine. **(F)** 5 mM pyruvic acid.

SI Table 3 Apparent binding constants determined with HQS emission. F_{max}, F_{min}, and K_{HQS} are determined by fitting HQS emission in the absence of chelators and used to calculate the free Mg^{2+} concentration in each sample. Metabolite binding constants, K' and K_D'. are determined by fitting the relationship between the free Mg^{2+} concentration and the total $MgCl_2$ concentration using SI Equation 4.

Metabolite	F_{max}	F_{min}	K_{HQS} (mM^{-1})	K' (mM^{-1})	K_D' (mM^{-1})
L-Glutamic acid	187,000 (1000)	0 (810)	0.281 (0.008)	0.0019 (0.0002)	520 (50)
Glutathione	182,000 (1000)	592 (750)	0.279 (0.007)	NA[c]	NA[c]
L-Aspartic acid	196,000 (1000)	0 (820)	0.283 (0.007)	0.0021 (0.0001)	465 (12)
L-Valine	188,200 (800)	495 (580)	0.274 (0.005)	NA[c]	NA[c]
L-Glutamine	190,000 (1400)	516 (110)	0.27 (0.01)	NA[c]	NA[c]
Pyruvic acid	188,000 (1500)	0 (1300)	0.35 (0.01)	0.063 (0.003)	15.8 (0.9)

[c]No binding observed as per SI Figure 2

SI Table 3. HQS fits in the absence of chelators, used to determine free Mg2+ concentrations. F_{max}, F_{min}, and K_{HQS} are determined by fitting HQS emission in the absence of chelators and used to calculate the free Mg^{2+} concentration in each sample.

Metabolite	F_{max}	F_{min}	K_{HQS} (mM^{-1})
Eco80	185,100 (800)	124 (1000)	0.239 (0.005)
NTPCM	187,000 (1500)	436 (1000)	0.26 (0.01)
WMCM	179,000 (1600)	0 (1400)	0.32 (0.01)

Table 2. Total Mg^{2+} concentrations used to obtain 2 mM free Mg^{2+} in artificial cytoplasm.

Condition	Total [Mg^{2+}] (mM)	Chelated [Mg^{2+}] (mM)	Free [Mg^{2+}] (mM)
Eco80	31.6	29.6	2.0
NTPCM	25.0	23	2.0
WMCM	6.4	4.5	2.0

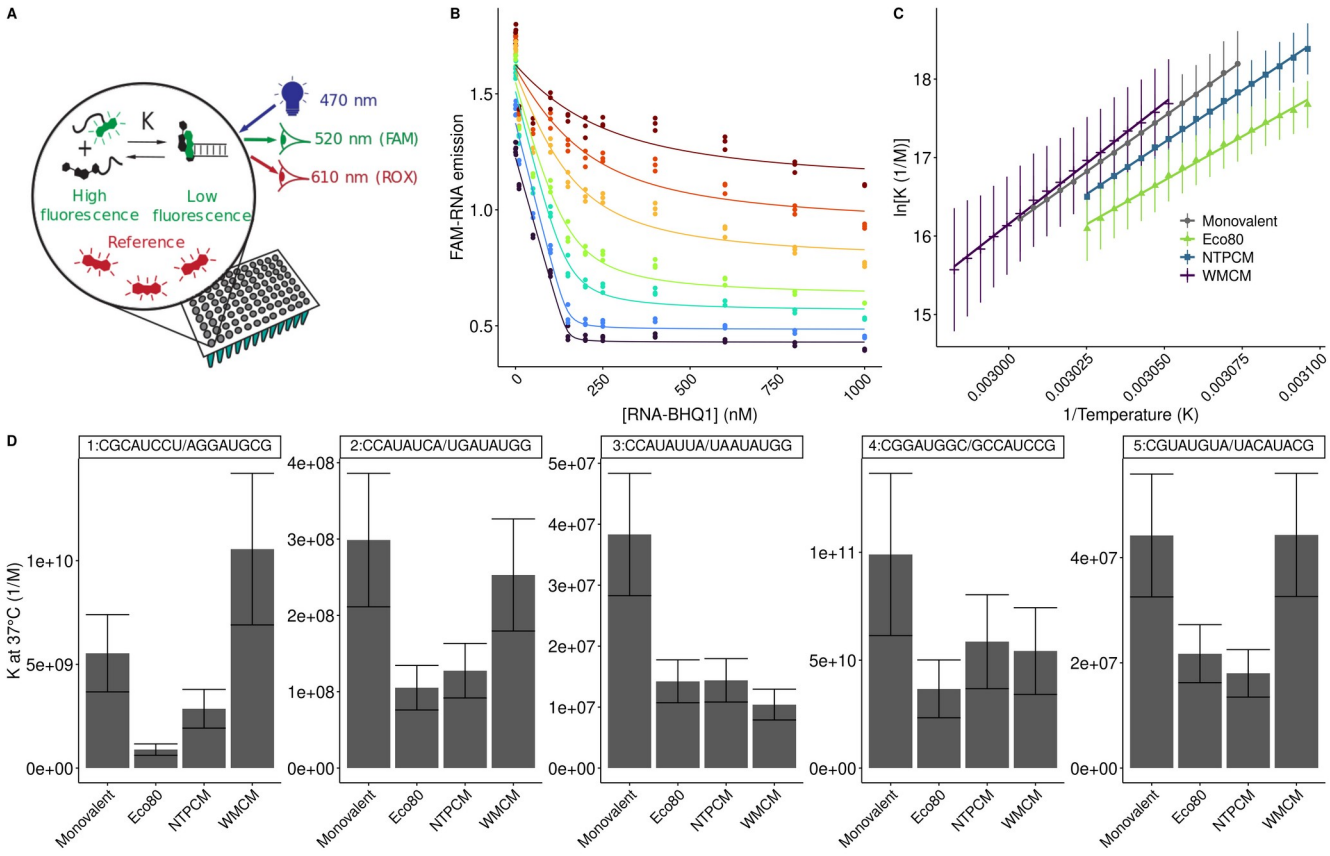

Figure 2 *E. coli* metabolite and Mg^{2+} mixtures destabilize RNA secondary structure. Helix folding energies in Eco80, NTPCM, and WMCM were determined using fluorescence binding isotherms that are fit with the MeltR program. **(A)** Layout of a fluorescence binding isotherms assay to determine helix folding energies in Eco80, NTPCM, and WMCM, in a Real-Time PCR machine. **(B)** Raw fluorescence binding isotherms fit to determine equilibrium constants with MeltR. Data points represent raw data. Curves represent curve fits. Colors represent different temperatures (purple: 32.3, blue: 41.8, teal: 51.3, green: 54.6, yellow: 58.4, orange: 60.7, red: 63.1 °C). **(C)** Van't Hoff relationship between equilibrium constant and temperature for helix 1:CGCAUCCU/AGGAUGCG folding in background monovalent metal ions (240 mM NaCl 140 mM KCl), Eco80, NTPCM, and WMCM. All conditions contain 2 mM free Mg^{2+}. Points and error bars represent association constants and standard errors propagated from the fit (using MeltR). Lines represent the fits to the Van't Hoff equation that MeltR uses to calculate folding energies. The y-axis uses the associations constant (K) instead of the disassociation constant (K_D) because Ks are proportional to stability. $K = 1/K_D$. A shift in the Van't Hoff relationship, down and to the right of the plot area, indicates that Eco80 destabilizes the Helix. **(D)** The association constant (K) at 37 °C in Eco80, NTPCM, and WMCM compared to the K at 37 °C in background monovalent metal ions (240 mM NaCl 140 mM KCl), for five RNA helices. All conditions contain 2 mM free Mg^{2+}. Errors were propagated assuming 1% uncertainty in the Gibb's free energy at 37 °C.

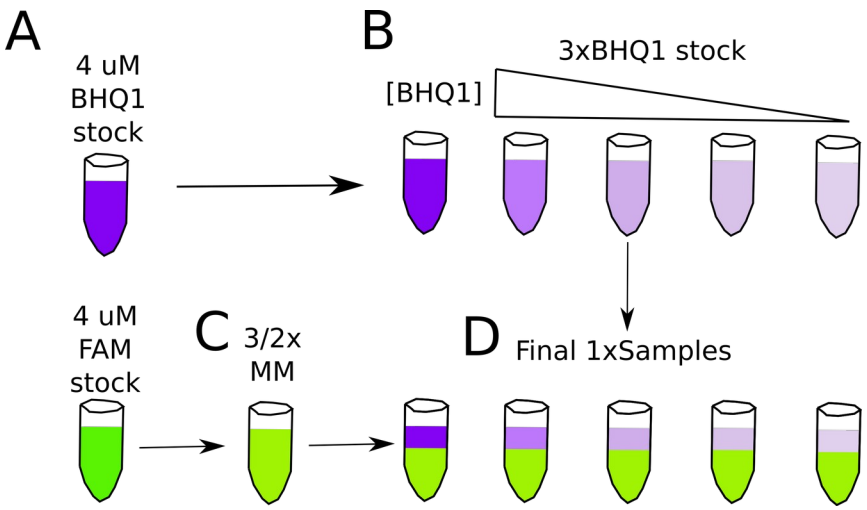

SI figure 3 Errors in the determination of concentrations of RNA stocks are systematically propagated during sample prep for fluorescence isotherm experiments. **(A)** FAM-RNA and RNA-BHQ1 stock concentrations are determined at a low μM concentrations with UV-absorbance. In this work, FAM and BHQ1 stocks were prepared at the same concentration, 4 μM. **(B)** RNA-BHQ1 stocks are diluted to a 3x concentration from one stock. **(C)** FAM-RNA stocks were diluted to a 3/2xconcentration into artificial cytoplasm to make a master mix (MM). **(D)** One volume of 3xRNA-BHQ1 stock is mixed with two volumes of 3/2xMM to prepare the final solution.

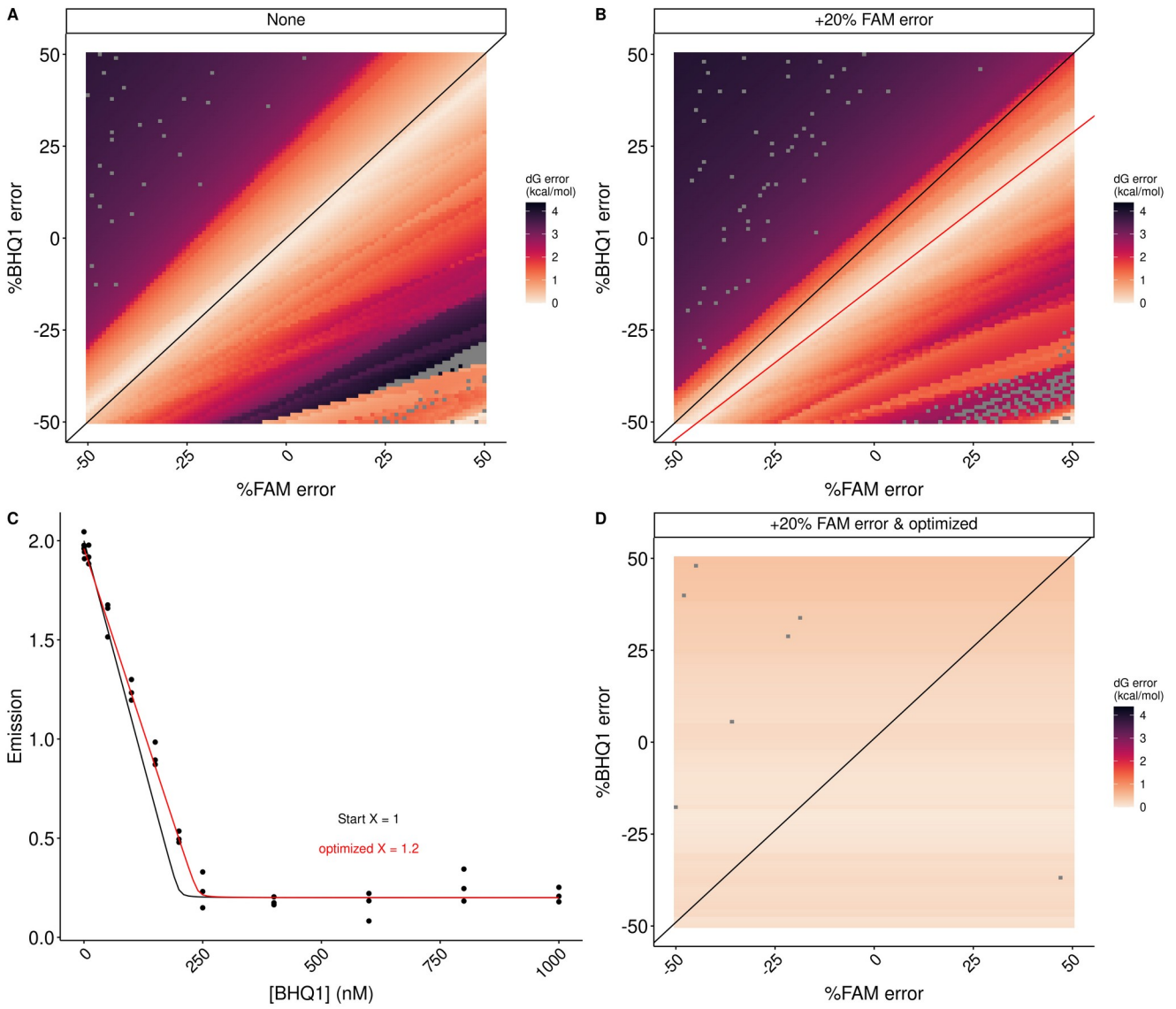

SI figure 4 The concentration optimization algorithm improves the accuracy of helix folding energies calculated with MeltR using data with inaccurate RNA concentration estimates. **(A)** Error in the Gibbs free energy (dG) calculated with MeltR on modeled data assuming perfectly accurate RNA concentration estimates is reduced when the %FAM-RNA concentration error and %RNA-BHQ1 concentration error compensates according to the black line, %FAM-RNA error = %RNA-BHQ1. Data were modeled assuming a folding enthalpy (ΔH), entropy (ΔS), and Gibb's free energy at 37 °C (ΔG) of -56.2 kcal/mol, -136. 4 cal/mol/K, and -13.9 kcal/mol respectively, and 5% random fluorescence error. Concentration errors were seeded into the modeled data and the data was fit with MeltR. **(B)** Error in the Gibbs free energy (dG) calculated with MeltR on modeled data, assuming a +20% FAM-RNA concentration estimate, is reduced when the %FAM-RNA concentration error and %RNA-BHQ1 concentration error compensate according to the red line, %RNA-BHQ1 = X*%FAM-RNA error + (100 – 100*X)/X, where X is the factor the MeltR concentration optimization algorithm multiplies the FAM-RNA concentration estimate by. Data were modeled assuming a folding ΔH, ΔS, and ΔG of -56.2 kcal/mol, -136. 4 cal/mol/K, and -13.9 kcal/mol respectively, 5% random fluorescence error, and a +20% increase in the FAM-RNA concentration. Additional concentration errors were seeded into the modeled data and the data was fit with MeltR. **(C)** MeltR identifies the FAM-RNA concentration correction factor (X) using a low temperature fluorescence isotherm as a Job plot. Black data points represent modeled fluorescence data from B at 20 °C. The black line represents the shape of the curve with a X of 1. The red line represents the shape of the curve with an optimized X of 1.2. **(D)** Error in the Gibbs free energy (dG) calculated with MeltR using the concentration optimization algorithm and the data from B. On average, MeltR estimates the correct ΔG within 0.2 kcal/mol, using the concentration optimization algorithm.

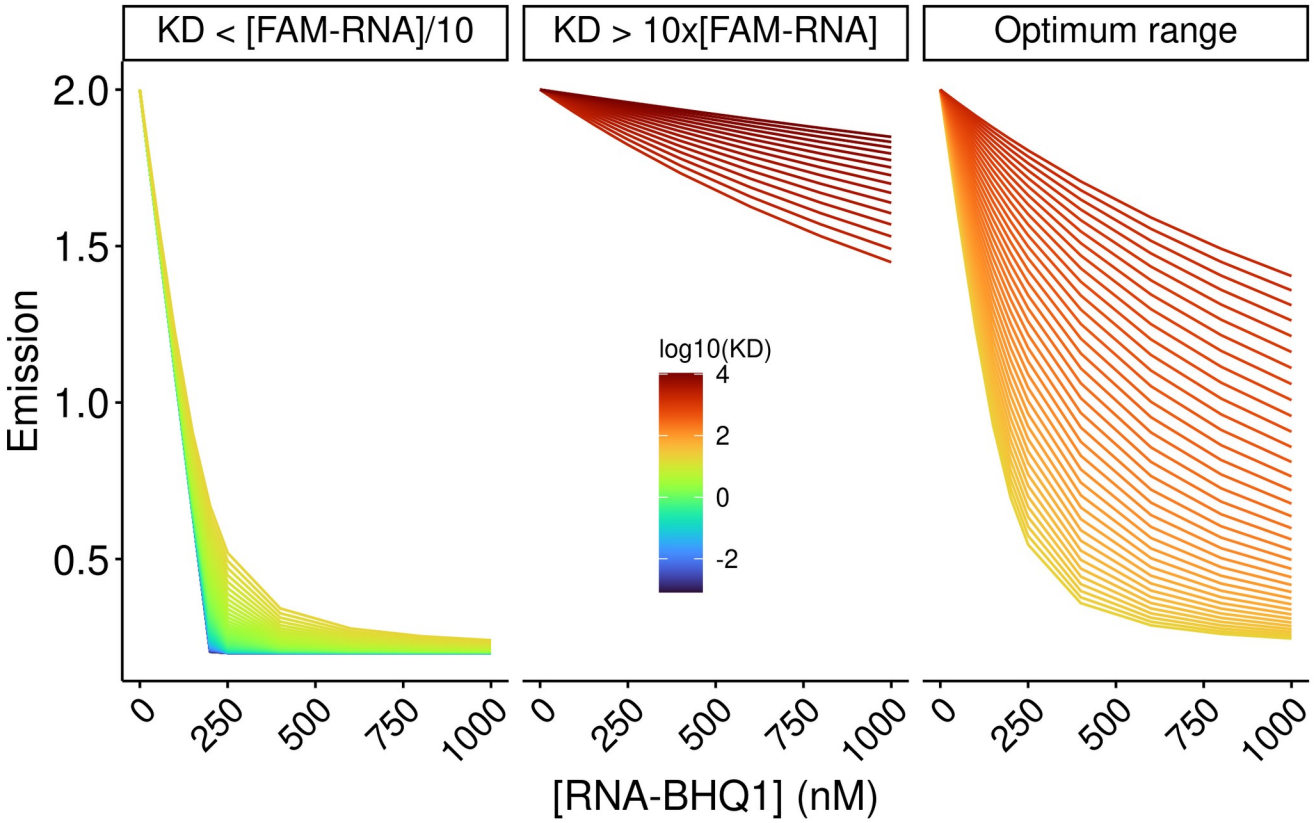

SI figure 5 K_Ds calculated using MeltR are most accurate between the FAM-RNA concentration/10 and 10 times the FAM-RNA concentration. At K_Ds that are more than 10 fold lower than the FAM-RNA concentration, the shape of the curve is independent of the K_D. At K_Ds more than 10 fold higher than the FAM-RNA concentration, there is very little dependence of FAM-RNA emission on RNA-BHQ1 concentration. However, the curve shape is highly dependent on K_D within the optimum range, so MeltR allows the user to specify an optimum K_D range to calculate helix folding energies.

SI table 4. Stability of RNA helices in *E. coli* metabolite mixtures. Helix energy was calculated by fitting raw fluorescence data with MeltR. Standard errors are estimated from fits. Extra significant digits are included to avoid propagating rounding errors.

Sequence[a]	Condition[b]	X[e]	Method 1 VH plot ΔH kcal/mol	Method 1 VH plot ΔS cal/mol/K	Method 1 VH plot ΔG kcal/mol	Method 2 Global fit ΔH kcal/mol	Method 2 Global fit ΔS cal/mol/K	Method 2 Global fit ΔG kcal/mol	%Diff.[d] ΔG	%Diff.[d] ΔS	%Diff.[d] ΔG
1:CGCAUCCU/ AGGAUGCG	2 mM free	1.3	-55.9 (0.2)	-136.0 (0.7)	-13.82 (0.01)	-56.0 (8.9)	-135.9 (27.0)	-13.8 (0.5)	0.2%	0.1%	0.1
	NTPCM	2	-52.2 (0.4)	-125 (1)	-13.41 (0.02)	-52.4 (7.6)	-125.6 (23.2)	-13.4 (0.4)	0.4%	0.5%	0.1%
	WMCM	1.0	-61.4 (0.8)	-152 (2)	-14.22 (0.05)	-61.1 (14.0)	-151.2 (42.5)	-14.2 (0.9)	0.5%	0.5%	0.1%
	Ecoli80	1.5	-44.5 (0.7)	-102 (2)	-12.70 (0.04)	-44.4 (7.6)	-102.1 (23.3)	-12.7 (0.4)	0.2%	0.1%	0.0%
2: CCAUAUCA/ UGAUAUGG	2 mM free	0.9	-53.4 (1.0)	-133 (3)	-12.02 (0.04)	-52.3 (14.9)	-129.9 (43.2)	-12.0 (0.5)	2.1%	2.4%	0.2%
	NTPCM	1.3	-42.9 (0.5)	-101 (1)	-11.50 (0.02)	-42.4 (20.4)	-99.6 (63)	-11.5 (0.8)	1.2%	1.4%	0.0%
	WMCM	1.0	-53 (2)	-132 (7)	-11.9 (0.1)	-51.6 (5.3)	-128.0 (1.6)	-11.9 (0.2)	2.7%	3.1%	0.0%
	Ecoli80	0.9	-57 (2)	-146 (5)	-11.38 (0.05)	-54.0 (13.1)	-137.7 (-41.1)	-11.3 (0.4)	5.4%	5.9%	0.7%
3:CCAUAUUA/ UAAUAUGG	2 mM free	0.9	-53.5 (0.4)	-137 (1)	-10.76 (0.01)	-53.2 (8.4)	-136.7 (27.1)	-10.8 (0.1)	0.6%	0.2%	0.4%
	NTPCM	1.0	-45.0 (0.2)	-112.5 (0.5)	-10.158 (0.002)	-45.0 (8.0)	-112.2 (25.6)	-10.2 (0.1)	0.0%	0.3%	0.4%
	WMCM	0.8	-43 (2)	-107 (5)	-9.94 (0.02)	-40.5 (9.3)	-98.4 (29.6)	-9.9 (0.1)	6.0%	8.4%	0.4%
	Ecoli80	1.2	-41.3 (0.2)	-100.4 (0.7)	-10.15 (0.01)	-41.2 (9.2)	-100.3 (29.4)	-10.2 (0.2)	0.2%	0.1%	0.5%
4:CGGAUGGC/ GCCAUCCG	2 mM free	1.1	-71.1 (0.8)	-179 (2)	-15.6 (0.06)	-71.3 (15.6)	-179.6 (46.6)	-15.6 (1.1)	0.3%	0.3%	0%
	NTPCM	1.2	-70.4 (0.6)	-177 (2)	-15.28 (0.05)	-70.5 (15.1)	-178.0 (45.2)	-15.3 (1.0)	0.1%	0.6%	0.1%
	WMCM	1.1	-65.5 (2)	-162 (7)	-15.2 (0.2)	-65.3 (12.2)	-161.6 (36.4)	-15.2 (0.9)	0.3%	0.2%	0%
	Ecoli80	1.0	-69.7 (0.8)	-176 (3)	-15.0 (0.1)	-69.6 (11.4)	-176.3 (34.2)	-15.0 (0.8)	0.1%	0.2%	0.2%
5:CGUAUGUA/ UACAUACG	2 mM free	0.8	-63.2 (0.9)	-169 (3)	-10.85 (0.02)	-62.3 (7.3)	-165.9 (23.0)	-10.8 (0.1)	1.4%	1.9%	0.5%
	NTPCM	0.9	-59 (1)	-157 (4)	-10.30 (0.01)	-58.5 (7.6)	-155.5 (24.3)	-10.3 (0.1)	0.9%	1.0%	0.0%
	WMCM	1.0	-67 (1)	-180 (3)	-10.85 (0.02)	-66.1 (10.5)	-178.1 (33.2)	-10.8 (0.2)	1.4%	1.1%	0.1%
	Ecoli80	1.0	-61 (1)	-164 (3)	-10.41 (0.01)	-60.9 (4.09)	-162.9 (13.1)	-10.4 (0.06)	0.2%	0.7%	0.2%
Average %error			1.7%	2.0%	0.3%	21.7%	26.5%	3.4%	1.2%	1.4%	0.2%

[a]The first sequence was 5'-FAM labeled and the second sequence was 3'-BHQ1 labeled.
[b]All solutions contain 2 mM Free Mg, 240 Na^+ 140 mM K^+.
[c]Concentration optimization factor used to correct FAM-RNA concentrations by MeltR.
[d]Percent difference between Method 1 and Method 2.

Table 3. Stability of RNA helices in *E. coli* metabolite mixtures.

Sequence[a]	AU content	Condition[b]	ΔG (kcal/mol)[c]	ΔΔG (kcal/mol)[c]
1: CGCAUCCU/ AGGAUGCG	0.38	2 mM free	-13.82 (0.21)	
		NTPCM	-13.41 (0.20)	0.41 (0.29)
		WMCM	-14.22 (0.21)	-0.40 (0.30)
		Ecoli80	-12.70 (0.19)	1.12 (0.28)
2: CCAUAUCA/ UGAUAUGG	0.63	2 mM free	-12.02 (0.18)	
		NTPCM	-11.50 (0.17)	0.52 (0.25)
		WMCM	-11.90 (0.18)	0.12 (0.25)
		Ecoli80	-11.38 (0.17)	0.64 (0.25)
3:CCAUAUUA/ UAAUAUGG	0.75	2 mM free	-10.76 (0.16)	
		NTPCM	-10.16 (0.15)	0.60 (0.22)
		WMCM	-9.94 (0.15)	0.82 (0.22)
		Ecoli80	-10.15 (0.15)	0.61 (0.22)
4: CGGAUGGC/ GCCAUCCG	0.25	2 mM free	-15.60 (0.23)	
		NTPCM	-15.28 (0.23)	0.32 (0.33)
		WMCM	-15.20 (0.23)	0.40 (0.33)
		Ecoli80	-15.00 (0.23)	0.60 (0.32)
5: CGUAUGUA/ UACAUACG	0.63	2 mM free	-10.85 (0.16)	
		NTPCM	-10.30 (0.15)	0.55 (0.22)
		WMCM	-10.85 (0.16)	0.00 (0.23)
		Ecoli80	-10.41 (0.16)	0.44 (0.23)

[a]The first sequence was 5'-FAM labeled and the second sequence was 3'-BHQ1 labeled.
[b]All solutions contain 2 mM Free3 Mg, 240 Na^+ 140 mM K^+.
[c]Extra significant digits were included to avoid propagating rounding errors.

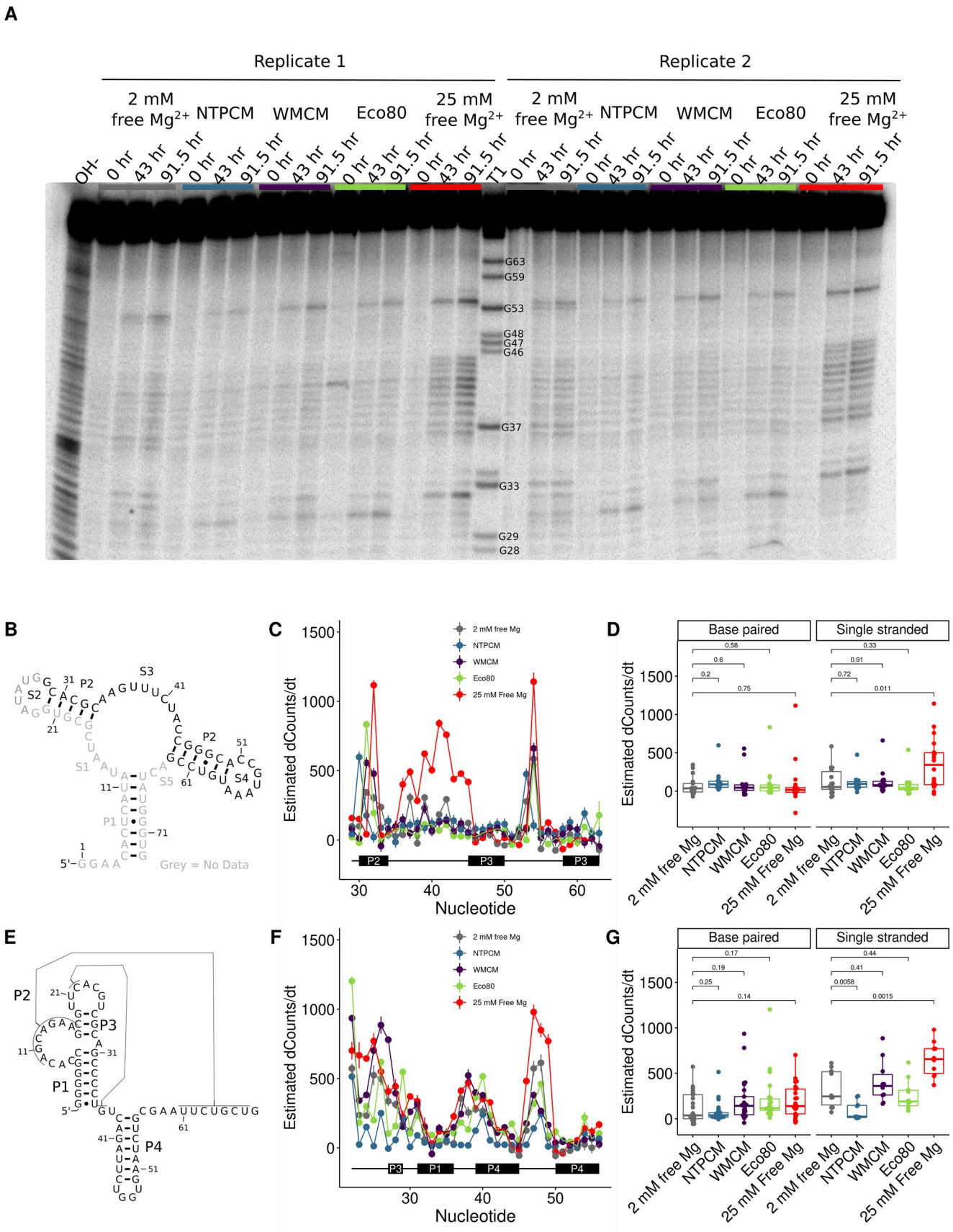

Figure 3 *E. coli* metabolite and Mg^{2+} mixtures stabilize the chemical structure of RNA. **(A)** Raw degradation assay gel image for the Guanine riboswitch aptamer incubated in artificial cytoplasms at 37 °C and pH 7. The

OH- lane contains a hydrolysis ladder which cleaves after every nucleotide and T1 contains the RNA treated with T1 ribonuclease which cleaves after every G. Enough Mg^{2+} was added to each artificial cytoplasm to have 2 mM Mg^{2+} as determined in Figure 1. **(B)** Secondary structure of the guanine riboswitch aptamer. **(C)** Estimated increase in counts as a function of time at each residue in different solution conditions as a function of location in the RNA. **(D)** Estimated increase in counts as a function of time in different conditions grouped by paired and unpaired bases. Significance was determined using a student's t-test. **(E)** Secondary structure of the cleaved human CPEB3 HDV ribozyme. **(C)** Estimated increase in counts as a function of time at each residue in different solution conditions as a function of location in the RNA. **(D)** Estimated increase in counts as a function of time in different conditions grouped by paired and unpaired bases. Significance was determined using a student's t-test.

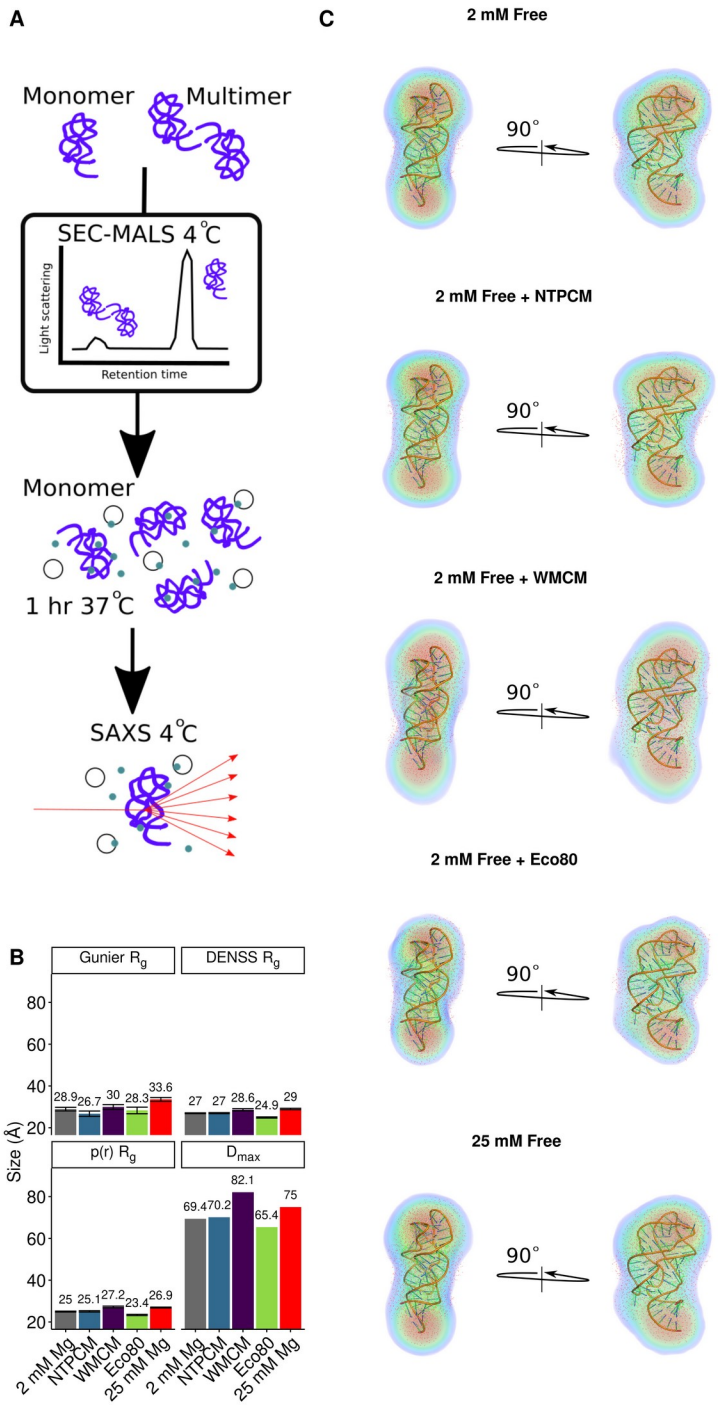

Figure 4 *E. coli* metabolite and Mg^{2+} mixtures increase functional RNA compactness.